Inverse modelling to reduce crosstalk in high density surface electromyogram

Inverse modelling to reduce crosstalk in high density surface electromyogram

Luca Mesin[a,*]

[a] *Mathematical Biology and Physiology, Dept. Electronics and Telecommunications, Politecnico di Torino, Turin, Italy*

Word count - 5400, 4000 (without references), 3500 (without references and figure captions)

Abstract

Surface electromyogram (EMG) has a relatively large detection volume, so that it could include contributions both from the target muscle of interest and from nearby regions (i.e., crosstalk). This interference can prevent a correct interpretation of the activity of the target muscle, limiting the use of surface EMG in many fields. To counteract the problem, selective spatial filters have been proposed, but they reduce the representativeness of the data from the target muscle. A better solution would be to discard only crosstalk from the signal recorded in monopolar configuration (thus, keeping most information on the target muscle). An inverse modelling approach is here proposed to estimate the contributions of different muscles, in order to focus on the one of interest. The method is tested with simulated monopolar EMGs from superficial nearby muscles contracted at different force levels (either including or not model perturbations and noise), showing statistically significant improvements in information extraction from the data. The median over the entire dataset of the mean squared error in representing the EMG of the muscle under the detection electrode was reduced from 11.2% to 4.4% of the signal energy (5.3% if noisy data were processed); the median bias in conduction velocity estimation (from 3 monopolar channels aligned to the muscle fibres) was decreased from 2.12 to 0.72 m/s (1.1 m/s if noisy data were processed); the median absolute error in the estimation of median frequency was reduced from 1.02 to 0.67 Hz in noise free conditions and from 1.52 to 1.45 Hz considering noisy data.

Keywords: Surface EMG, Crosstalk, Inverse Problem, Source Localization

1. INTRODUCTION

The relatively large pick-up volume of surface electromyogram (EMG) has been considered as a limitation with respect to invasive alternatives, which could provide more selective information [1][2]. However, recording contributions from a large region, surface EMG can represent the overall activity of a great portion of the muscle. The only

*Corresponding author
Email address: luca.mesin@polito.it (Luca Mesin)

problem is discriminating the sources of the recorded signal. In particular, it is important to focus on the activity of interest, removing the crosstalk produced by nearby muscles. The interference may originate from muscles which are located either adjacent (e.g., vastus medialis and lateralis [3]), or deeper (ankle flexors and extensors [4], soleus and gastrocnemius [5]), or around the target muscle (forearm muscles [6][7]). The problems introduced by crosstalk were documented in different applications: gait analysis [8], muscle coordination [9], ergonomics [6], reflexes [10], prosthetic control [11] and many others [12][13].

The biophysical origin and the quantification of crosstalk have been investigated in different conditions, using both simulations [14][15] and experiments [3][16][17][18][19][20]. The main key for understanding it is related to the shape variations of motor unit (MU) action potentials (MUAP) as they are recorded from different locations. Specifically, current sources propagating along muscle fibres provide near-field potentials, whereas their generations and extinctions produce far-field contributions. Thus, the surface EMG produced by the same sources has different shape when recorded from different sites, as each MUAP is constituted by contributions that vary differently with distance. For this reason, crosstalk cannot be simply quantified by cross-correlating the signals recorded over the target and the crosstalk muscles [21].

In particular, crosstalk is usually due to the activity of muscles which are located farther from the detection electrodes than the target one and it is thus mainly constituted by generation and extinction effects. These contributions are sharp when recorded close to the bioelectric source, but they are smoothed by the volume conductor as they are recorded far from it. As a result, crosstalk bandwidth is superimposed to that of the target EMG, so that temporal filters are not beneficial to reduce it [22].

Far-field effects are similar when recorded by different electrodes, on the contrary of the contributions of the propagating sources. For this reason, placing a linear array of electrodes aligned to the fibres of the target muscle, propagating and non-propagating components can be recorded [23]: the first contributions allow to investigate muscle fibre conduction velocity (CV, an important EMG index, e.g., to investigate muscle pathology or fatigue [24]), whereas the second ones induce a bias in CV estimation [25]. As mentioned above, crosstalk is mainly constituted by far-field/non-propagating components, thus inducing a bias in CV estimation from the target muscle.

In applications, crosstalk is usually reduced using selective spatial filters [17][26]. However, the optimal filter depends on the specific tissues [14][15], so that it should be estimated by adapting to the specific condition [25]. Moreover, selective filters discard not only crosstalk, but also the signal from the target muscle, recording data which are less representative of its activity [5], which could be a problem when studying a muscle providing multiple biomechanical actions [27].

Thus, monopolar data include most information from the target muscle, but they are the most affected by crosstalk; on the other hand, optimal selective filters can reduce crosstalk, but they provide poor information on the target muscle. Hence, reducing crosstalk from monopolar data could be a useful alternative to the use of spatial filters, which has the advantage of keeping most information from the target muscle.

In this paper, the signals produced by the target and the crosstalk muscles are estimated by inverse modelling. The method is used to quantify and reduce crosstalk. Monopolar EMGs are considered, in order to extract most of the information from the target muscle. The possibility of compensating for the bias introduced by crosstalk in

estimating EMG amplitude, CV and median frequency (MDF) of the target muscle is investigated.
This work is an extension of a preliminary congress contribution [28].

2. Methods

2.1. Inverse modelling algorithm

Surface EMG is the electric potential over the skin induced by bioelectric currents flowing across the membrane of muscle fibres and inducing their contraction. Identifying the active regions in a muscle from the recorded EMG is an inverse problem. In general, inverse problems are difficult to solve, as they require to estimate the cause (the current sources in our case), given the effect (i.e., the surface EMG). The direct problem of surface EMG simulation can be simulated solving an electrostatic problem [29] (assumption valid if voluntary contractions are considered [30]), with Poisson equation relating the bioelectric source and the potential distribution in the tissues, thus, in particular, over the skin surface. This problem was extensively studied for surface electroencephalogram (EEG) [31], e.g., with the aim of supporting presurgical evaluation of epileptic patients [32]. Most of the methods proposed in the field of surface EMG have a high computational cost, as they either require to apply intensive simulations by the finite elements method (FEM)[33] or to decompose the interference EMG into constituent MUAPs [34].

Here, a low cost method is considered, which could even be run in real-time [35]. It is based on an interpretation model, to be inverted to fit the data, which are assumed to be approximately represented as a linear combination of a set of single fibre action potentials (SFAP), each representing the activity of a source in a specific location (assuming the action potential to propagate at 4 m/s along muscle fibres):

$$b\left(x,t\right)=\sum_{n=1}^{N_R}\sum_{k=1}^{N_\tau}X_{n,k}a_n\left(x,t-\tau_{nk}\right) \tag{1}$$

where $b\left(x,t\right)$ is the EMG, x is the space variable (indicating the position of the recording channels), t is the time variable, τ_{nk} is a delay (N_τ is the number of considered delays) and $a_n(x,t)$ are N_R basis waveforms (i.e., the SFAPs representing the activity of a source located in a specific region). The coefficients $\{X_{n,k}\}$ are the unknowns and indicate the activity of a specific source (the n^{th}) at a certain time (i.e., corresponding to the delay τ_{nk}). Notice that this interpretation model is quite coarse in approximating a real EMG, e.g., as only few basis waveforms are considered (instead of hundreds of MUAPs generated by the MUs involved in a high level contraction), their shape cannot be exactly equal to any MUAP (indeed, they are only SFAPs), the details of the volume conductor and fibres anatomy could be not known precisely, a constant value of muscle fibre CV was considered, and electrical noise was not included.

As shown in [35], Equation (1) can be rewritten in matrix form

$$AX=b, \tag{2}$$

with the basis waveforms (with all considered delays) placed in the columns of the matrix A, the vector b including the measurements and X collecting the unknowns. Due to model

approximations, experimental noise and the inherent instability of the inverse problem, a least mean squared solution was sought after introducing Tikonov regularization [35]

$$\min_X \|AX - b\|^2 + \alpha \|X\|^2 \tag{3}$$

where the first term is the residual norm (measuring the error in data fitting) and the second is the solution norm (weighted by α equal to one thousandth of the maximum eigenvalue of the matrix $A^T A$), imposing the energy of the solution to be small (avoiding oscillating solutions with large phase cancellations; on the other hand, the essential solution including only few sources is selected, accepting a larger residual variance in fitting the data, with such a residual error ideally reflecting the contribution of noise). The problem has the following analytical solution

$$X = (A^T A + \alpha I)^{-1} A^T b \tag{4}$$

2.2. Simulated EMGs for tests

The same generation model as in [28] was used, but extensive simulations were here performed. In brief, the volume conductor and electrode configuration are shown in Figure 1. Two nearby muscles were considered, each including 400 MUs uniformly distributed in their cross-sections. Their MUAPs were simulated by summing simulated SFAPs in monopolar configuration (10 fibres per mm^2, MU centres chosen randomly and closest fibres selected as belonging to them).

The basis waveforms used for the fitting model (1) were 90 in total, distributed in the muscle cross-section, with depth between 1 and 9 mm (2 mm step) and angle between $\pm 45^o$ (5^o step, removing 0^o, which is the angle of the plane separating the two muscles).

For each muscle, interference EMGs of 20 s duration were simulated (as in [36]) for contraction levels in the range 5-100% of the maximal voluntary contraction (MVC; 5% step) and combined to generate the dataset to test the algorithm (parameters used to generate the interference signals: range of recruitment thresholds 70% of MVC; range of the firing rate 8–30 Hz, with linear increase with the force level with slope of 1 Hz per 1% MVC, after MU recruitment and until the upper limit of the firing rate; 10% random Gaussian jitter of the inter-spike interval).

Both ideal and noisy conditions were considered. In the first case, the basis waveforms were simulated using the same volume conductor model as the one considered to simulate the test EMGs (as in the representative simulations shown in [28]). In the tests in noisy conditions, the same simulated EMGs were corrupted by adding white Gaussian noise with 25 dB of signal-to-noise ratio. High frequency noise was then attenuated by a lowpass filter with cutoff 350 Hz (6^{th} order Chebychev filter of type I, applied twice, once with time reversed to remove phase distortion). Moreover, the volume conductor used to simulate the basis waveforms for inverse modelling included the following differences with respect to the one used to generate the test signals: the cylindrical volume conductor had a radius 2 mm larger, the fat layer was 1 mm thinner, the skin was twice thicker, the diameter of the bone was 5 mm shorter and the conductivities of all tissues were the 50% larger.

2.3. Performance evaluation

The following performance measurements were used to check the accuracy of the proposed algorithm.

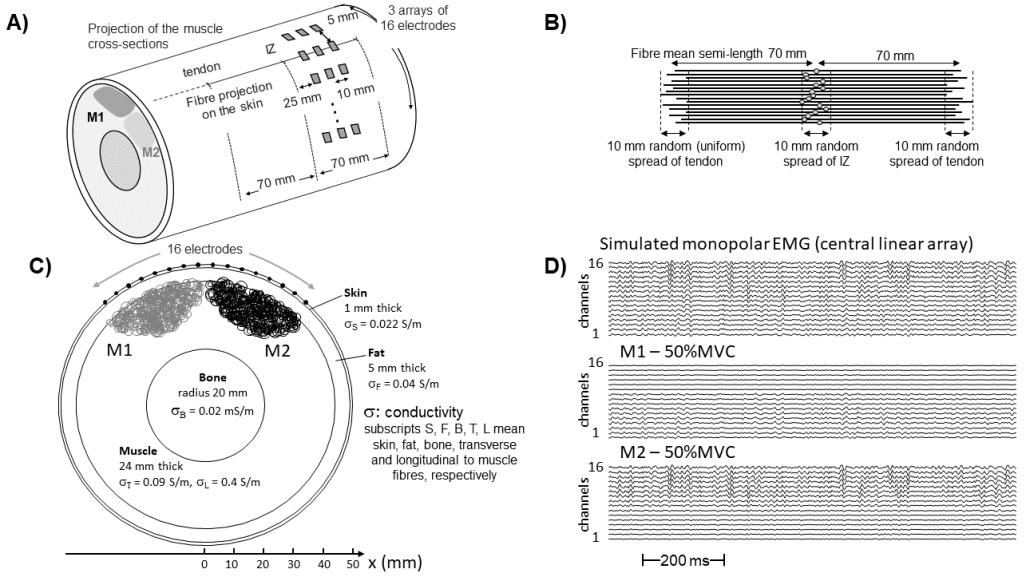

Figure 1: Description of the simulation model. A) Cylindrical volume conductor used to simulate two muscles (M1 and M2). Monopolar signals were acquired from a grid of electrodes of 16 rows and 3 columns (transverse and parallel to the muscle fibres, respectively). B) Indication of the anatomy of the muscle fibres. C) Cross-section of the volume conductor with indication of the location and dimension of the motor units (400 for each muscle). D) Example of simulated monopolar signal, showing the raw EMG and the contribution of each of the two muscles recorded by a linear array in the transverse direction with respect to the muscle fibres.

- Mean squared error (MSE) in the estimation of the simulated signal from each of the two muscles recorded over it, given in terms of percentage with respect to the energy

$$MSE(f_1, f_2, x) = 2\frac{\int\limits_t (s_{f_1,f_2}(x,t) - \tilde{s}_{f_1,f_2}(x,t))^2 dt}{\int\limits_t s^2_{f_1,f_2}(x,t)dt + \int\limits_t \tilde{s}^2_{f_1,f_2}(x,t)dt} \tag{5}$$

  where s and $\tilde{s}$ are the simulated and estimated EMG signals, respectively, produced by the muscle under the considered channel. These signals depend on the force level f_k of muscle Mk (with $k = 1, 2$), the location of the electrodes x and time t.

- The ratio of the RMS amplitudes of the surface EMG of a muscle (either simulated or estimated) over the total EMG was used to provide a quantification of crosstalk

$$R(f_1, f_2, x) = \frac{\|m_{f_1,f_2}(x,t)\|_2}{\|T_{f_1,f_2}(x,t)\|_2} \tag{6}$$

  where m is the signal produced by a single muscle, T is the total EMG (sum of the contributions of the two muscles, either simulated or estimated) and $\|\cdot\|_2$ is the L_2 norm obtained integrating over time. The performance in the quantification of crosstalk was measured in terms of the mean absolute difference of the ratio R obtained using as signal m either the simulated or the estimated EMG from the considered muscle.

- Muscle fibre CV is biased by crosstalk. It was estimated on the raw EMG and on those produced by the muscle under the electrodes, either simulated or estimated. The estimation was obtained by applying the multi-channel spectral matching algorithm [37] to the three monopolar signals aligned to the muscle fibres, for each of the 16 transverse location shown in Figure 1A and 1C (80 epochs of 250 ms). The performance of the proposed algorithm was measured in terms of the mean absolute error in estimating CV from the muscle under the electrodes.

- Spectral parameters are biased by crosstalk. Median frequency (MDF) was estimated considering the sample spectrum computed on 20 epochs of 1 s duration of the monopolar signal detected from the central electrode of each triplet aligned to muscle fibres. To overcome resolution problems (limiting to 1 Hz the estimation accuracy), after computing the MDF on the sample spectrum, the two closest points were interpolated with a quadratic polynomial to refine the estimation. MDF was computed on the raw EMG and on that produced by the muscle under the electrodes, either simulated or estimated. The performance of the proposed algorithm was measured in terms of the mean absolute error in estimating MDF from the muscle under the electrodes.

The indexes were functions of the force levels of the two muscles and of the location of the electrodes. They were shown either as a function of the force levels of the two muscles (computing the median across channels) or of the channel (showing the distributions of values depending on the force levels).

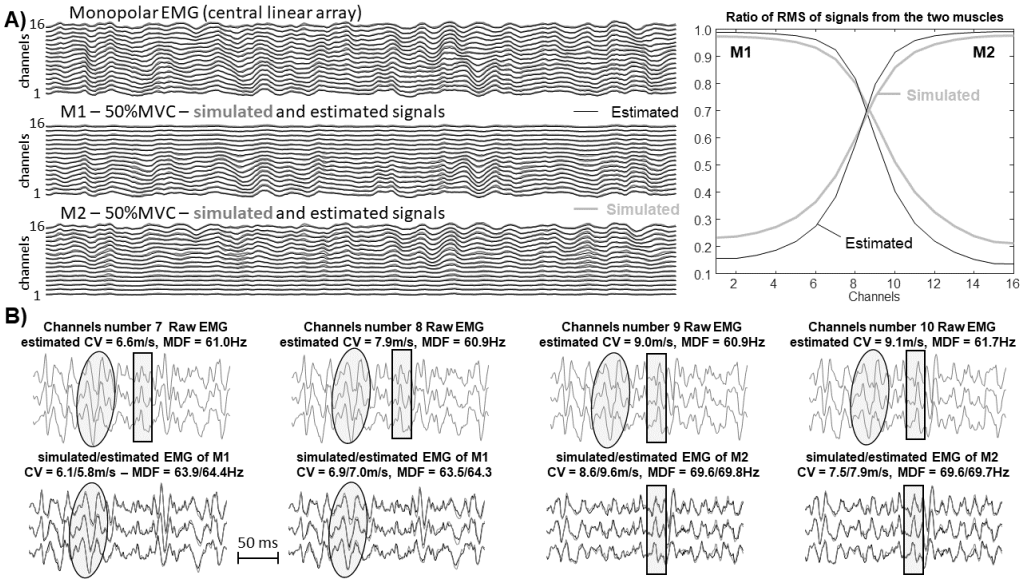

Figure 2: Example of signal processing to estimate the contributions of the two muscles. A) Examples of signals: total EMG and contributions of either of the two muscles. Simulated and estimated signals are superimposed (mean squared errors, defined in equation (5), in the estimation of the contributions of M1 and M2 were 7.2% and 6.4%, respectively). Quantification of muscle crosstalk, in terms of the percentage of RMS of signals from the two muscles (central linear array in transverse direction). B) Example of estimation of muscle fibre conduction velocity (CV, from the shown 250 ms epoch) and median frequency (MDF, from 1 s epoch centred on the shown one) from either the raw EMG or the signals obtained after removing the contributions of the crosstalk muscles (i.e., the simulated/estimated signal of M2 was removed from channels 1-8, that of M1 from channels 9-16). A portion of data from the central columns of electrodes is shown (both raw data and simulated/estimated contributions of the muscles under the electrodes). Some MUAPs are indicated using ellipsoids and rectangles: they are visible from all channels in the raw signal, but they are produced by either of the two muscles.

3. Results

Figures 2-5 show the accuracy of the proposed method in quantifying crosstalk and reducing its effect in the considered simulated data. Some representative examples of processing are first shown, then overall results on the entire dataset are presented, proving the possibility of reducing the bias in amplitude, CV and MDF estimation.

Figure 2 shows an example of EMG processing. A signal including contributions of the two muscles at 50% of their MVC is considered. The percentage RMSs of the two muscles over the transverse position are shown in 2A, comparing simulated and estimated signals. This test indicates the potential application in the quantification of the contributions of crosstalk (shown on the right). Moreover, a bias in amplitude estimation from the target muscle could be compensated (as further assessed in the following Figure 3). Figure 2B shows an example of estimation of CV and MDF of the target muscle (i.e., the one under the considered electrodes). Some portions of signals from the central channels are shown: notice that some MUAPs are visible in all channels, but they should be considered either as signal or as crosstalk (e.g., the MUAPs indicated with ellipses and rectangles are visible in all channels, but they are produced by either M1 or M2,

respectively). The algorithm, by discriminating the contributions of the two muscles, can be used to remove the crosstalk contribution (i.e., the signal from the muscle which is not under the electrodes). This can reduce the bias in CV and MDF estimation. However, the algorithm is efficient only if the crosstalk muscle is not too close: some problems are expected in the channels number 8 and 9 (actually, only for channel 9 the bias in CV estimation is not reduced, whereas MDF measurement was always improved in the specific example shown in the figure). In fact, consider that they are only 2.5 mm distant from the plane separating the two muscles (i.e., $x = 0$ in Figure 1C). Moreover, the resolution of the sources of the kernel waveforms is quite poor: it is about one source every 5.5 mm^2, with a mean transverse distance between closest sources of about 3.4 mm. The problems in discriminating the signals from the two muscles hamper the estimation of EMG indexes from those channels which are very close to the crosstalk muscle. Consider also that in such channels the contribution of crosstalk is mainly constituted by propagating components of MUAPs generated by MUs close to the electrodes. On the other hand, most crosstalk found in the other channels is due to non-propagating components (related to generation and extinction of action potentials). The removal of such contributions is very important to reduce the bias in CV and MDF estimation in all other channels (as further shown in the following Figures 4 and 5).

Figure 3 shows overall results on amplitude estimation, considering all simulations. The MSE in estimating the contributions of the two muscles is shown in 3A as a function of their force levels. The median MSE decreased from 11.2% of the signal energy (using raw data) to 4.4 % (using processed data; processing noisy data, the median MSE was 5.3%). Notice that a larger mistake is obtained when the force level of the target muscle is small and that of the crosstalk muscle is big. The mean absolute error in crosstalk quantification is shown in 3B, considering M1 as target muscle. Notice that the best estimation is found when the two muscles have similar force levels (e.g., if the force contribution of a muscle is not lower than the 30% of the other, the average error is lower than 10%). The error in estimating the EMG of the target muscle is shown in Figure 3C as a function of the electrode location in the transverse direction. Notice that the algorithm allows to reduce the estimation error in all locations, even considering noisy processed data compared to noise free raw EMGs.

Figure 4 shows the results of CV estimation obtained considering the entire dataset. The absolute error in estimating CV from the target muscle (i.e., M1 for channels 1-8, M2 for channels 9-16) is shown as a function of the force level in 4A and 4B, after computing the median across channels, considering the raw and processed data, either including or not the noise perturbations. The median bias in CV estimation of the muscle under the electrode decreased from 2.12 m/s (using raw data) to 0.72 m/s (using processed data; processing noisy data, the bias was 1.1 m/s). Notice that removing crosstalk is important when the force levels are not much different. The absolute error in CV estimation is shown in 4C as a function of the detection channels (for each channel, the distribution of the 400 combinations of force levels is displayed). As already noticed in Figure 2B for a specific case, when removing the estimated contributions of crosstalk, CV computation could be degraded for channels 8 and 9 (i.e., the closest to $x = 0$). For all other channels, crosstalk removal is beneficial to improve CV estimation.

Figure 5 shows the results of MDF estimation obtained considering the entire dataset. As for the estimation of CV mentioned above, the absolute error from the target muscle (i.e., M1 for channels 1-8, M2 for channels 9-16) is shown as a function of the force level

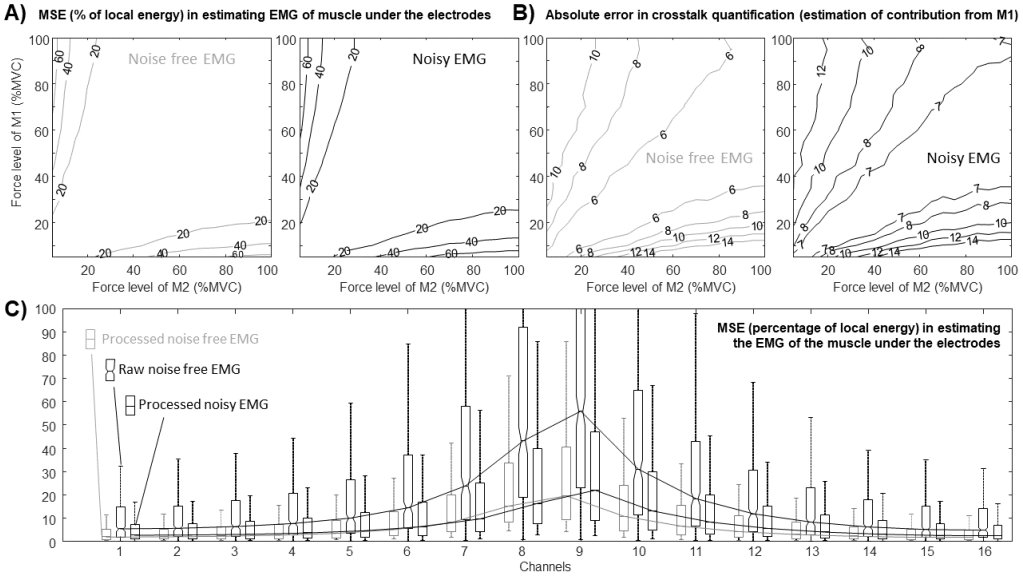

Figure 3: Collective results from simulations of different contraction levels: for each muscle, contraction levels in the range 5-100%MVC (5% step) were considered. A) MSE in estimating the contributions of each muscle (averaging across channels and time samples), normalized by the average energy of the simulated and estimated signals. B) Mean absolute error in quantifying muscle crosstalk as the percentage of energy of the signal from muscle M1 (central linear array in transverse direction). C) Distribution of MSE (shown in terms of median, quartiles and range) of the estimation of the EMG of the target muscle (i.e., the one under the electrode) as a function of the transverse location of the detection point. For each electrode location, Wilcoxon signed rank test indicated statistical differences between raw and processed data (either corrupted or not by noise).

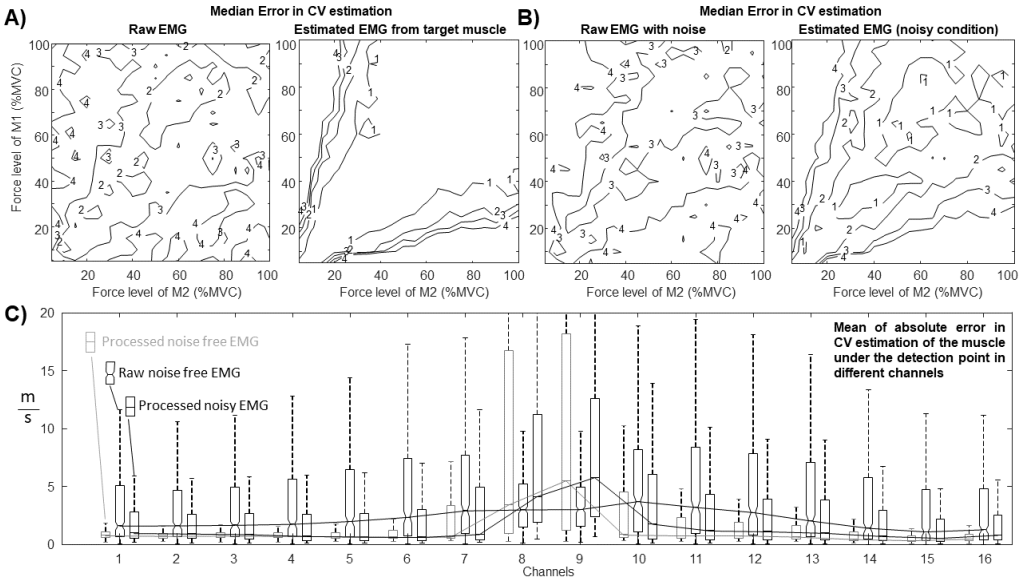

Figure 4: Collective results of CV estimation considering simulations of different contraction levels. A) Median (over channels) of mean absolute error in the estimation of the CV of the muscle under the electrodes using either the raw data or the EMG processed to remove the estimated contribution of the crosstalk muscle, as a function of the contraction levels of the two muscles. B) Same as A), but considering noisy data. C) Distribution (considering different contraction levels) of mean absolute error in estimating CV of the signal of the muscle under the electrodes, considering either the raw EMG or the one obtained after removing the estimated crosstalk (with or without noise corruption). The distributions of errors are shown in terms of median, quartiles and range. Wilcoxon signed rank test indicated statistical differences between raw and processed data (either corrupted or not by noise) for each electrode location.

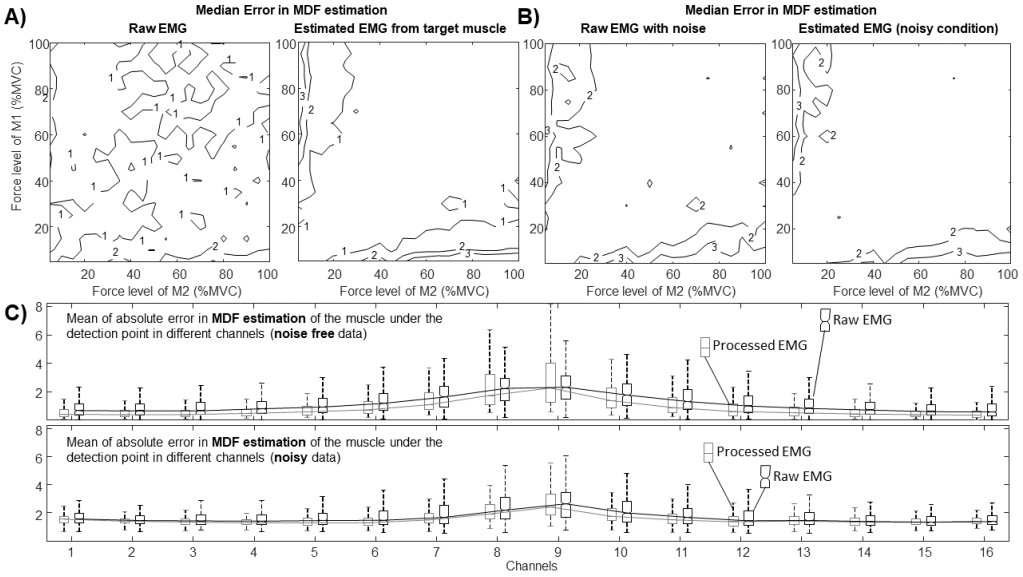

Figure 5: Collective results of MDF estimation considering simulations of different contraction levels. The central electrode of each triplet aligned to the muscle fibres was considered. A) Median (over channels) of mean absolute error in the estimation of the MDF of the muscle under the electrodes using either the raw data or the EMG processed to remove the estimated contribution of the crosstalk muscle, as a function of the contraction levels of the two muscles. B) Same as A), but considering noisy data. C) Distribution (considering different contraction levels) of mean absolute error in estimating MDF of the signal of the muscle under the electrodes, considering either the raw EMG or the one obtained after removing the estimated crosstalk (with or without noise corruption). The distributions of errors are shown in terms of median, quartiles and range. Wilcoxon signed rank test indicated statistical differences between raw and processed data for each location except for electrode 10 for noise free data and electrode 6 for noisy data.

in 5A and 5B (median across channels), considering the raw and processed data, either including or not the noise perturbations. The median bias in the estimation of MDF of the target muscle (i.e., that under the electrode) decreased from 1.02 Hz to 0.67 Hz using respectively raw and processed noise free data. In noisy conditions, the median absolute error was 1.52 Hz for the raw signal and 1.45 Hz for the processed data. Again, removing crosstalk is important when the force levels are not much different. The distribution of the absolute error in MDF estimation (over the force levels) as a function of the detection channels is shown in Figure 5C. The median bias is always quite small, but larger for the electrodes closer to the crosstalk muscle. However, there is always a lower median of the estimation errors when using the processing method to reduce crosstalk (with statistically significant improvements of the performances in all but few cases).

4. Discussion

The applications of surface EMG can be limited by crosstalk from muscles placed nearby the target one [2][6][8][9][10][11][12]. Indeed, crosstalk may be misinterpreted as signal produced by the muscle of interest, affecting the extraction of different information

from it, e.g., activation intervals, EMG amplitude, spectral content and muscle fibre CV. Even though the problems induced by crosstalk are well-known, no standard methodology is accepted to measure or reduce its contribution. The most common approach to reduce it relies on recording the EMG by selective spatial filters. However, optimal filters should be adapted to the investigated anatomy [15] and they provide information only on a small detection volume, which could be not representative of the overall activity of the target muscle [5].

Here a different method is explored, i.e., estimating the contributions of the target and crosstalk muscles, in order to remove the interference and being able to better extract the information of interest. The method is tested on simulations from close superficial muscles. Discriminating the two contributions is an inverse problem, which is inherently unstable. Indeed, MUAPs generated by close sources are very similar, so that the discrimination is quite difficult, in particular when the crosstalk muscle is contracted at a much higher force level than the target one and the detection channel is close to both. Moreover, the model used to fit the data includes some coarse approximations: the number of considered sources (90) is quite limited with respect to the simulated MUs (800), as it should be in the order of the number of electrodes sensing the EMG (48); the kernel waveforms of the inverse model were simulated with a constant CV equal to 4 m/s. The effect of further problems like additive noise or differences between the volume conductor used to simulate the basis waveforms and the EMG were investigated in [35], showing that the method is quite stable in the identification of the transverse location of the active regions, which is useful to identify crosstalk from nearby superficial muscles. More tests were performed here, confirming that the estimation of crosstalk is stable to additive noise and problems in the volume conductor model. Indeed, the estimation of the amplitude and CV of the target muscle improved even comparing noise free raw data and EMG processed in noisy conditions. The MDF was largely affected by the additive noise (and also by the filter used to remove the contributions out of EMG bandwidth): however, improvements in estimating it were observed comparing raw data either noise free or noisy and their processed versions, respectively. As already noticed in [28], the best estimations are obtained when the two muscles have similar force levels.

These promising results indicate the need of further tests in experimental conditions. In such a case, the level of crosstalk is not known a-priori (only tests in simulations allow to overcome this problem). However, more stable estimations of amplitude, MDF and CV from the target muscle are expected during the co-activation of a crosstalk muscle when using the proposed processing method. Moreover, experimental signals from selective activations of different muscles could be combined to simulate a co-contraction. Thus, some quantitative tests of the performances of the method could be investigated even in experimental conditions.

The present study has the limitation of considering a specific simulation model. Close parallel muscles were simulated. This is a condition in which the inverse modelling approach has shown stable results [35]. Other interesting geometrical configurations could be studied, e.g., crosstalk could come from a deep muscle (more difficulties are expected in such a condition, as the depth of sources is difficult to be estimated with good accuracy [35]). Moreover, fibre orientation could be different, e.g., pinnate muscles could be investigated. Further investigation in those directions is suggested.

5. Conclusions

Crosstalk is a subtle problem which can limit the application of surface EMG in many fields. There's no standard for its quantification and reduction. In this paper, an inverse modelling approach is proposed to address the quantification and reduction of crosstalk. Tests in simulations show promising results in estimating its contribution and in reducing the bias in amplitude, MDF and CV estimation.

Acknowledgments

Competing interests: None declared
Funding: None
Ethical approval: Not required

References

[1] M. Besomi, P. Hodges, J. Van Dieën, R. Carson, E. Clancy, C. Disselhorst-Klug, A. Holobar, F. Hug, M. Kiernan, M. Lowery, K. McGill, R. Merletti, E. Perreault, K. Søgaard, K. Tucker, T. Besier, R. Enoka, D. Falla, D. Farina, S. Gandevia, J. Rothwell, B. Vicenzino, T. Wrigley, Consensus for experimental design in electromyography (cede) project: Electrode selection matrix, Journal of Electromyography and Kinesiology 48 (2019) 128–144. doi:10.1016/j.jelekin.2019.07.008.

[2] A. Péter, E. Andersson, A. Hegyi, T. Finni, O. Tarassova, N. Cronin, H. Grundstrom, A. Arndt, Comparing surface and fine-wire electromyography activity of lower leg muscles at different walking speeds, Frontiers in Physiology 10 (2019) 1283. doi:10.3389/fphys.2019.01283.

[3] D. Farina, R. Merletti, B. Indino, M. Nazzaro, M. Pozzo, Surface emg crosstalk between knee extensor muscles: experimental and model results, Muscle Nerve 26 (2002) 681–695. doi:10.1002/mus.10256.

[4] C. D. Luca, R. Merletti, Surface myoelectric signal crosstalk among muscles of the leg, Clin. Neurophysiol. 69 (1988) 568–575. doi:10.1016/0013-4694(88)90169-1.

[5] T. Vieira, A. Botter, S. Muceli, D. Farina, Specificity of surface emg recordings for gastrocnemius during upright standing, Sci Rep. 7 (2017) 13300. doi:10.1038/s41598-017-13369-1.

[6] Y.-K. Kong, M. S. Hallbeck, M.-C. Jung, Crosstalk effect on surface electromyogram of the forearm flexors during a static grip task, Journal of Electromyography and Kinesiology 20 (6) (2010) 1223–1229. doi:10.1016/j.jelekin.2010.08.001.

[7] J. Mogk, P. Keir, Crosstalk in surface electromyography of the proximal forearm during gripping tasks, Journal of Electromyography and Kinesiology 13 (1) (2003) 63–71. doi:10.1016/S1050-6411(02)00071-8.

[8] K. M. Barr, A. L. Miller, K. B. Chapin, Surface electromyography does not accurately reflect rectus femoris activity during gait: Impact of speed and crouch on vasti-to-rectus crosstalk, Gait & Posture 32 (3) (2010) 363–368. doi:10.1016/j.gaitpost.2010.06.010.

[9] F. Hug, Can muscle coordination be precisely studied by surface electromyography?, Journal of Electromyography and Kinesiology 21 (1) (2011) 1–12. doi:10.1016/j.jelekin.2010.08.009.

[10] R. A. Mezzarane, A. F. Kohn, A method to estimate emg crosstalk between two muscles based on the silent period following an h-reflex, Medical Engineering & Physics 31 (10) (2009) 1331–1336. doi:10.1016/j.medengphy.2009.09.005.

[11] N. Jiang, K. Englehart, P. Parker, Extracting simultaneous and proportional neural control information for multiple-dof prostheses from the surface electromyographic signal, IEEE Trans Biomed Eng. 56 (1) (2009) 1070–1080. doi:10.1109/TBME.2008.2007967.

[12] I. Talib, K. Sundaraj, C. Lam, J. Hussain, M. Ali, A review on crosstalk in myographic signals, Eur J Appl Physiol. 119 (2019) 9–28. doi:10.1007/s00421-018-3994-9.

[13] L. Mesin, Crosstalk in surface electromyogram: literature review and some insights, Phys Eng Sci Med. (2020). doi:10.1007/s13246-020-00868-1.

[14] L. Mesin, Simulation of surface emg signals for a multilayer volume conductor with a superficial bone or blood vessel, IEEE Trans Biomed Eng 25 (2008) 1647–1657. doi:10.1109/TBME.2008.919104.

[15] L. Mesin, S. Smith, S. Hugo, S. Viljoen, T. Hanekom, Effect of spatial filtering on crosstalk reduction in surface emg recordings, Medical Engineering & Physics 31 (3) (2009) 374–383. doi:10.1016/j.medengphy.2008.05.006.

[16] I. Campanini, A. Merlo, P. Degola, R. Merletti, G. Vezzosi, D. Farina, Effect of electrode location on emg signal envelope in leg muscles during gait, Journal of Electromyography and Kinesiology 17 (4) (2007) 515–526. doi:10.1016/j.jelekin.2006.06.001.

[17] D. Farina, L. Arendt-Nielsen, R. Merletti, B. Indino, T. Graven-Nielsen, Selectivity of spatial filters for surface emg detection from the tibialis anterior muscle, IEEE Trans. Biomed. Eng. 50 (2003) 354–364. doi:10.1109/TBME.2003.808830.

[18] D. Farina, C. Févotte, C. Doncarli, R. Merletti, Blind separation of linear instantaneous mixtures of nonstationary surface myoelectric signals, IEEE Trans. Biomed. Eng. 51 (2004) 1555–1567. doi:10.1109/TBME.2004.828048.

[19] R. Merletti, C. D. Luca, D. Sathyan, Electrically evoked myoelectric signals in back muscles: Effect of side dominance, J. Appl. Physiol. 77 (1994) 2104–2114. doi:10.1152/jappl.1994.77.5.2104.

[20] M. Solomonow, R. Baratta, M. Bernardi, B. Zhou, Y. Lu, M. Zhu, S. Acierno, Surface and wire emg crosstalk in neighbouring muscles, Journal of Electromyography and Kinesiology 4 (3) (1994) 131–142. doi:10.1016/1050-6411(94)90014-0.

[21] M. Lowery, N. Stoykov, T. Kuiken, A simulation study to examine the use of cross-correlation as an estimate of surface emg cross talk, Journal of Applied Physiology 94 (2003) 1324–1334. doi:10.1152/japplphysiol.00698.2002.

[22] N. Dimitrova, G. Dimitrov, O. Nikitin, Neither high-pass filtering nor mathematical differentiation of the emg signals can considerably reduce cross-talk, Journal of Electromyography and Kinesiology 12 (4) (2002) 235–246. doi:10.1016/S1050-6411(02)00008-1.

[23] L. Mesin, Separation of interference surface electromyogram into propagating and non-propagating components, Biomedical Signal Processing and Control 52 (2019) 238–247. doi:10.1016/j.bspc.2019.04.016.

[24] L. Mesin, D. Dardanello, A. Rainoldi, G. Boccia, Motor unit firing rates and synchronisation affect the fractal dimension of simulated surface electromyogram during isometric/isotonic contraction of vastus lateralis muscle, Med. Eng. & Phys. 38 (2016) 1530–1533. doi:10.1016/j.medengphy.2016.09.022.

[25] L. Mesin, Optimal spatio-temporal filter for the reduction of cross-talk in surface electromyogram, J Neural Eng. 15 (2018) 016013. doi:10.1088/1741-2552/aa8f03.

[26] C. J. D. Luca, M. Kuznetsov, L. D. Gilmore, S. H. Roy, Inter-electrode spacing of surface emg sensors: Reduction of crosstalk contamination during voluntary contractions, Journal of Biomechanics 45 (3) (2012) 555–561. doi:10.1016/j.jbiomech.2011.11.010.

[27] A. Gallina, A. Botter, Spatial localization of electromyographic amplitude distributions associated to the activation of dorsal forearm muscles, Frontiers in Physiology 4 (2013) 367. doi:10.3389/fphys.2013.00367.

[28] L. Mesin, Quantification and reduction of crosstalk in surface electromyogram by inverse modelling, in: GNB2020 (VII Congress of the National Group of Bioengineering), 2020.

[29] L. Mesin, Volume conductor models in surface electromyography: Computational techniques, Comput. Biol. Med. 43 (7) (2013) 942–952. doi:10.1016/j.compbiomed.2013.02.002.

[30] L. Mesin, R. Merletti, Distribution of electrical stimulation current in a planar multilayer anisotropic tissue, IEEE Trans Biomed Eng. 55(2 Pt 1) (4) (2008) 660–670. doi:10.1109/TBME.2007.902248.

[31] C. M. Michel, D. Brunet, Eeg source imaging: A practical review of the analysis steps, Frontiers in Neurology 10 (2019) 325. doi:10.3389/fneur.2019.00325.

[32] M. Lopes, L. Junges, L. Tait, J. Terry, E. Abela, M. Richardson, M. Goodfellow, Computational modelling in source space from scalp eeg to inform presurgical evaluation of epilepsy, Clinical Neurophysiology 131 (2020) 225–234. doi:10.1016/j.clinph.2019.10.027.

[33] K. van den Doel, U. M. Ascher, D. K. Pai, Source localization in electromyography using the inverse potential problem, Inverse Problems 27 (2) (2011) 025008. doi:10.1088/0266-5611/27/2/025008.

[34] K. Roeleveld, D. Stegeman, H. Vingerhoets, A. V. Oosterom, The motor unit potential distribution over the skin surface and its use in estimating the motor unit location, Acta Physiologica Scandinavica 161 (4) (1997) 465–472. doi:10.1046/j.1365-201X.1997.00247.x.

[35] L. Mesin, Real time identification of active regions in muscles from high density surface electromyogram, Comput. Biol. Med. 56 (C) (2015) 37–50. doi:10.1016/j.compbiomed.2014.10.017.

[36] A. Fuglevand, D. Winter, A. Patla, Models of recruitment and rate coding organization in motor-unit pools, J. Neurophysiol. 70 (1993) 2470–2488. doi:10.1152/jn.1993.70.6.2470.

[37] D. Farina, W. Muhammad, E. Fortunato, O. Meste, R. Merletti, H. Rix, Estimation of single

motor unit conduction velocity from surface electromyogram signals detected with linear electrode arrays., Medical and Biological Engineering and Computing 39 (2) (2001) 225–236. doi:10.1007/BF02344807.